Inorganic Chemistry

Article

pubs.acs.org/IC

# Metal-Controlled Assembly of Uranyl Diphosphonates toward the Design of Functional Uranyl Nanotubules

Pius O. Adelani and Thomas E. Albrecht-Schmitt*

Department of Civil Engineering and Geological Sciences and Department of Chemistry and Biochemistry, University of Notre Dame, Notre Dame, Indiana 46556, United States

Supporting Information

**ABSTRACT:** Two uranyl nanotubules with elliptical cross sections were synthesized in high yield from complex and large oxoanions using hydrothermal reactions of uranyl salts with 1,4-benzenebisphosphonic acid or 4,4′-biphenylenbisphosphonic acid and $Cs^+$ or $Rb^+$ cations in the presence of hydrofluoric acid. Disordered $Cs^+/Rb^+$ cations and solvent molecules are present within and/or between the nanotubules. Ion-exchange experiments with $A_2\{(UO_2)_2F(PO_3HC_6H_4C_6H_4PO_3H)(PO_3HC_6H_4C_6H_4PO_3)\}\cdot 2H_2O$ (A = $Cs^+$, $Rb^+$), revealed that $A^+$ cations can be exchanged for $Ag^+$ ions. The uranyl phenyldiphosphonate nanotubules, $Cs_{3.62}H_{0.38}[(UO_2)_4\{C_6H_4(PO_2OH)_2\}_3\{C_6H_4(PO_3)_2\}F_2]\cdot nH_2O$, show high stability and exceptional ion-exchange properties toward monovalent cations, as demonstrated by ion-exchange studies with selected cations, $Na^+$, $K^+$, $Tl^+$, and $Ag^+$. Studies on ion-exchanged single crystal using scanning electron microscopy and energy dispersive X-ray spectroscopy (SEM/EDS) provide evidence for chemical zonation in $Cs_{3.62}H_{0.38}[(UO_2)_4\{C_6H_4(PO_2OH)_2\}_3\{C_6H_4(PO_3)_2\}F_2]\cdot nH_2O$, as might be expected for exchange through a diffusion mechanism.

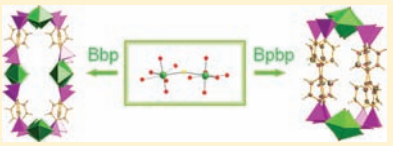


## INTRODUCTION

Early studies on the structural chemistry of U(VI) demonstrated the dominance of layered structures, especially among minerals, with diverse coordination environments for uranium that favor tetragonal, pentagonal, and hexagonal bipyramidal geometries in almost boundless combinations.[1] U(VI) coordination chemistry is exceptionally rich, and most compounds contain uranyl cations, $UO_2^{2+}$, and because of the generally inert nature of the two oxo atoms, it was assumed that three-dimensional network structures would be infrequent and that curvature (nanotubules and nanospheres) would be unusual.[2,3] However, recent advances in the synthetic and structural chemistry of U(VI) has yielded unprecedented shapes, topologies, and properties with potential applications in materials chemistry and waste management.[4] This field has indeed undergone a revolution with increasingly fascinating structural architectures such as nanotubules[2] and nanospheres,[3] which are assembled using organic linkers and U(VI) cations. Uranyl oxoanion materials have displayed important properties that include selective ion-exchange, ionic conductivity, intercalation chemistry, photochemistry, nonlinear optics, and catalysis.[5−8]

We are particularly interested in developing the solid-state chemistry of uranyl arylphosphonate compounds.[2a,9] Until recently, our understanding of the coordination chemistry of actinide arylphosphonates has been limited mostly to those of uranyl phenylphosphonate reported by Clearfield et al. and a handful of other compounds.[2g−k,10] The coordination chemistry of uranyl phenyldiphosphonate is very rich, displaying the first member in the family of uranyl nanotubules that was isolated via the transformation of one-dimensional $\alpha$- and $\beta$-uranyl phenylphosphonates upon exposure to $Na^+$ or $Ca^{2+}$ cations in aqueous solution.[2i,j] We have demonstrated in our previous reports that rigid phenyldiphosphonates can be used to construct pillared uranyl structures in the presence of organic amines as structure directing agents.[9b,c] When we replaced the aromatic amines with the $Cs^+$ cation to template the structure of a uranyl phenyldiphosphonate, a remarkable structure of $Cs_{3.62}H_{0.38}\{(UO_2)_4[C_6H_4(PO_2OH)_2]_3[C_6H_4(PO_3)_2]F_2\}\cdot nH_2O$ resulted. This compound possesses an elliptical uranyl nanotubular structure, and atypical ion-exchange properties where the cations on the interior of the tubes exchange much more rapidly than those on the exterior.[2a] The application of nanotubular structures in the uranyl system has been highlighted previously.[3c] Applications of nanotubular structures in ion-exchange studies have been partially reported by our group.[3b] The aim of this paper is to communicate further advances we have made to uncover new nanotubular topologies. As an extension of the previous work on phenyldiphosphonate, we have further expanded on this system by using 4,4′-biphenylenebisphosphonate as a linker between U(VI) centers, and present here in detail the syntheses, structural characterization, and ion-exchange properties of these compounds, $A_2\{(UO_2)_2F(PO_3HC_6H_4C_6H_4PO_3H)(PO_3HC_6H_4C_6H_4PO_3)\}\cdot 2H_2O$ (A = $Cs^+$, $Rb^+$) (**CsUbpbp-1** and **RbUbpbp-1**), and $Cs_{3.62}H_{0.738}\{(UO_2)_4[C_6H_4(PO_2OH)_2]_3[C_6H_4(PO_3)_2]F_2\}\cdot nH_2O$ (**CsUbbp-1**).

## EXPERIMENTAL SECTION

**Synthesis.** $UO_2(NO_3)_2\cdot 6H_2O$ (98%, International Bio-Analytical Industries), HF (48 wt %, Aldrich), 4,4′-biphenylenebisphosphonic acid (98%, Epsilon Chimie), 1,4-benzenebisphosphonic acid (95%, Epsilon Chimie), sodium chloride, potassium chloride, rubidium chloride, cesium chloride, thallium nitrate, silver nitrate, and strontium chloride hexahydrate (Alfa Aesar) were used as received. Reactions were run in PTFE-lined Parr 4749 autoclaves with a 23 mL internal

**Received:** September 5, 2011
**Published:** November 3, 2011

ACS Publications © 2011 American Chemical Society

volume. Distilled and Millipore filtered water with resistance of 18.2 MΩ·cm was used in all reactions.

***Caution!*** *While all the uranium compounds used in these studies contained depleted uranium salts, standard precautions were performed for handling radioactive materials, and all studies were conducted in a laboratory dedicated to studies on actinide elements.*

**$M_2\{(UO_2)_2F(PO_3HC_6H_4C_6H_4PO_3H)(PO_3HC_6H_4C_6H_4PO_3)\}\cdot 2H_2O$ ($M = Cs^+$ and $Rb^+$) (CsUbpbp-1 and RbUbpbp-1).** $UO_2(NO_3)_2\cdot 6H_2O$ (50.1 mg, 0.1 mmol), 4,4′-biphenylenebisphosphonic acid (63.0 mg, 0.2 mmol), CsCl (36.3 mg, 0.2 mmol) or RbCl (24.2 mg, 0.2 mmol), 0.7 mL of water, and HF (50 μL) were loaded into a 23 mL autoclave. The autoclave was sealed and heated to 200 °C in a box furnace for 5 days and was then cooled at an average rate of 3 °C/h to 25 °C. The resulting yellow product was washed with distilled water and methanol and allowed to air-dry at room temperature. Yellow platelets of **CsUbpbp-1** and needles of **RbUbpbp-1** were isolated in pure phase (Yields are **CsUbpbp-1** = 76% and **RbUbpbp-1** = 69%).

The preparation of $Cs_{3.62}H_{0.38}\{(UO_2)_4[C_6H_4(PO_2OH)_2]_3[C_6H_4(PO_3)_2]F_2\}\cdot nH_2O$ (**CsUbbp-1**) is described in ref 2a.

**Crystallographic Studies.** Single crystals of **CsUbpbp-1** and **RbUbpbp-1** were mounted on cryoloops and optically aligned on a Bruker APEXII Quazar CCD X-ray diffractometer using a digital camera. Initial intensity measurements were either performed using a standard sealed tube (Mo) with a monocapillary collimator. Standard APEXII software was used for determination of the unit cells and data collection control. The intensities of reflections of a sphere were collected by a combination of four sets of exposures (frames). Each set had a different $\varphi$ angle for the crystal and each exposure covered a range of 0.5° in $\omega$. A total of 1464 frames were collected with an exposure time per frame of 30 or 40 s, depending on the crystal size and quality. SAINT software was used for data integration including Lorentz and polarization corrections. Semiempirical absorption corrections were applied using the program SADABS.[11a] The program suite SHELXTL was used for space group determination (XPREP), direct methods structure solution (XS), and least-squares refinement (XL).[11b] The final refinements included anisotropic displacement parameters for all atoms except hydrogen. Selected crystallographic data are given in Tables 1−3. Atomic coordinates, bond distances, and additional structural information are provided in the Supporting Information (CIFs).

**Powder X-ray Diffraction (XRD).** Powder XRD patterns were collected on a Scintag $\theta-\theta$ diffractometer equipped with a diffracted-beamed monochromatic set for Cu K$\alpha$ ($\lambda$ = 1.5418 Å) radiation at room temperature in the angular range from 5° to 65° ($2\theta$) with a scanning step width of 0.05° and a fixed counting time of 1 s/step. The collected patterns were compared with those calculated from single-crystal data using ATOMS and Mercury (see Supporting Information).

**Spectroscopic Characterization.** Fluorescence and absorption data were acquired for the compounds from single crystals using a Craic Technologies UV−vis−NIR microspectrophotometer with a fluorescence attachment. The absorption data was collected in the range of 250−1200 nm at room temperature. The fluorescence spectra were recorded in the range of 450−650 nm at room temperature and excitation was achieved using 365 nm light from a mercury lamp for the fluorescence spectroscopy. Infrared spectra were collected from single crystals of the two compounds using a SensIR Technology IlluminatIR FT-IR microspectrometer. A single crystal of each compound was placed on a glass slide, and the spectrum was collected with a diamond ATR objective (see the Supporting Information).

**Thermogravimetric Analysis.** A TGA measurement was conducted on **CsUbpbp-1** and **RbUbpbp-1** using a Netzsch TG209 F1 Iris thermal analyzer for 10 mg of each sample in an $Al_2O_3$ crucible that was heated from 20 to 900 °C at a rate of 5 °C/min under flowing nitrogen gas. The data are shown in the Supporting Information.

**Scanning Electron Microscopy (SEM) and Energy Dispersive X-ray Spectroscopy (EDS) Analyses.** SEM/EDS images and data were collected using a LEO EVO 50 with an Oxford INCA Energy Dispersive Spectrometer. Samples were mounted on a carbon coated tape. The energy of the electron beam was 29.02 kV, and the spectrum acquisition time was 180 s. All of the data were calibrated with standards.

**Table 1. Crystallographic Data for $Cs_2\{(UO_2)_2F(PO_3HC_6H_4C_6H_4PO_3H)(PO_3HC_6H_4C_6H_4PO_3)\}\cdot 2H_2O$ (CsUbpbp-1) and $Rb_2\{(UO_2)_2F(PO_3HC_6H_4C_6H_4PO_3H)(PO_3HC_6H_4C_6H_4PO_3)\}\cdot 2H_2O$ (RbUbpbp-1)**

| | CsUbpbp-1 | Rbbpbp-1 |
|---|---|---|
| formula mass | 1477.05 | 1376.81 |
| color and habit | yellow, platelet | yellow, needles |
| space group | $P\bar{1}$ (No. 2) | $P\bar{1}$ (No. 2) |
| $a$ (Å) | 9.9997(10) | 9.8504(14) |
| $b$ (Å) | 10.6653(10) | 10.6472(15) |
| $c$ (Å) | 17.1456(16) | 16.799(2) |
| $\alpha$ (deg) | 86.364(1) | 86.172(2) |
| $\beta$ (deg) | 77.716(1) | 75.258(2) |
| $\gamma$ (deg) | 81.550(1) | 81.429(2) |
| $V$ (Å) | 1766.3(3) | 1684.1(4) |
| Z | 2 | 2 |
| $T$ (K) | 103 | 100 |
| $\lambda$ (Å) | 0.71073 | 0.71073 |
| $\rho_{calcd}$ (g cm$^{-3}$) | 2.777 | 2.715 |
| $\mu$ (Mo K$\alpha$) (mm$^{-1}$) | 11.45 | 12.75 |
| $R(F)$ for $F_o^2 > 2\sigma(F_o^2)^a$ | 0.022 | 0.026 |
| $Rw(F_o^2)^b$ | 0.053 | 0.057 |

$^aR(F) = \sum||F_o| - |F_c||/\sum|F_o|$. $^bR(F_0^2) = \sum w(F_o^2 - F_c^2)^2/\sum w(F_o^4)]^{1/2}$.

**Ion-Exchange Studies with CsUbpbp-1, RbUbpbp-1, and CsUbbp-1.** The ion-exchange properties of **CsUbpbp-1**, **RbUbpbp-1**, and **CsUbbp-1** were investigated with selected cations, using NaCl, KCl, $TlNO_3$, $AgNO_3$, and $SrCl_2$. A total of 15 mg of the crystals of **CsUbpbp-1**, **RbUbpbp-1**, and **CsUbbp-1** were placed in Teflon vials (8 mL), and 5 mL of a 5 M solution of respective metal salts were added and the vial were then covered. The solutions were mixed for several days with a mechanical shaker at room temperature, and for $TlNO_3$ at 70 °C with magnetic stirrer. The mixture was filtered with filter paper and the solids were air-dry at room temperature. Some of these crystals were mounted on the X-ray diffractometer for unit cell and/or structural determination, powder XRD, and subsequently for elemental analysis using EDS. Because of loss of crystallinity, most of the crystals isolated from **CsUbpbp-1** and **RbUbpbp-1** compounds after ion-exchange were only characterized further by powder XRD and EDS.

## RESULTS AND DISCUSSION

**Synthesis.** **CsUbpbp-1**, **RbUbpbp-1**, and **CsUbbp-1** can be prepared under mild hydrothermal conditions. HF has substantial effects on the reactions, and substantially affects crystallinity. It serves as both a mineralizing agent and ligand in all of these compounds.

**Structure of $A_2\{(UO_2)_2F(PO_3HC_6H_4C_6H_4PO_3H)(PO_3HC_6H_4C_6H_4PO_3)\}\cdot 2H_2O$ ($A = Cs^+$ and $Rb^+$).** The structures of both **CsUbpbp-1** and **RbUbpbp-1** are similar except that they contain different alkali metal cations. The structure of $A_2\{(UO_2)_2F(PO_3HC_6H_4C_6H_4PO_3H)(PO_3HC_6H_4C_6H_4PO_3)\}\cdot 2H_2O$ is different from previous members of this family that have nearly circular cross sections.[2b−l] This compound is similar to **CsUbbp-1** in that they are both nanotubular; **CsUbpbp-1** or **RbUbpbp-1** is highly elliptical with tube dimensions of approximate 1 × 1.5 nm compared to reported value of 1 × 2 nm in **CsUbbp-1** as shown in Figure 1.[2a] $Cs^+/Rb^+$ cations are seated inside the tubes in **CsUbbp-1** because of its larger size dimension compared to the smaller size dimension in **CsUbpbp-1**/**RbUbpbp-1** which is too small to accommodate alkali cations.


dx.doi.org/10.1021/ic201945p | Inorg. Chem. 2011, 50, 12184−12191

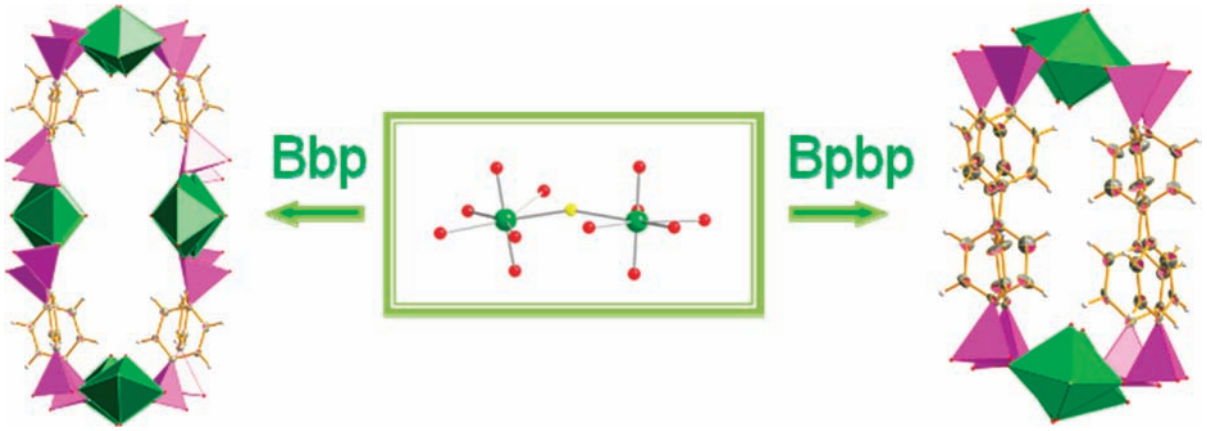


**Figure 1.** Views of the uranyl diphosphonates with elliptical nanotubular structure in $Cs_{3.62}H_{0.38}\{(UO_2)_4[C_6H_4(PO_2OH)_2]_3[C_6H_4(PO_3)_2]F_2\}\cdot nH_2O$ and $M_2\{(UO_2)_2F(PO_3HC_6H_4C_6H_4PO_3H)(PO_3HC_6H_4C_6H_4PO_3)\}\cdot 2H_2O$. The structure is constructed from $UO_6F$ pentagonal bipyramids = green, oxygen = red, phosphorus = pink, fluorine = yellow, carbon = gray, phenyl ring = orange, hydrogen = white.

The structure is composed of corner-sharing uranyl dimers of $UO_6F$, pentagonal bipyramids, that are linked through a fluoride anion, therefore making the inclusion of HF in the synthesis very important (see Figure 2a and 3). The

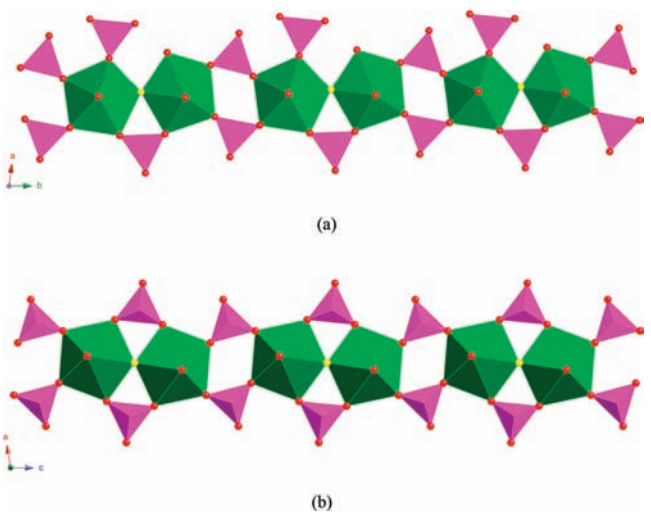


**Figure 2.** (a) Polyhedral representation of the uranyl-phosphate chain viewed along the *c* axis in $M_2\{(UO_2)_2F(PO_3HC_6H_4C_6H_4PO_3H)(PO_3HC_6H_4C_6H_4PO_3)\}\cdot 2H_2O$. (b) A Polyhedral view along the *b* axis showing the $UO_7$ dimers in $Cs_{3.62}H_{0.38}\{(UO_2)_4[C_6H_4(PO_2OH)_2]_3[C_6H_4(PO_3)_2]F_2\}\cdot nH_2O$. $UO_6F$ pentagonal bipyramids = green, oxygen = red, phosphorus = magenta, fluorine = yellow.

assignments of either F or O atoms were made based on the improvements in the refinements when the correct element was selected. Typically when the element was incorrectly identified the thermal parameters become nonpositive definite when refined anisotropically. Moreover, this is important to chemically balance the charge on the compound. This was further confirmed by SEM/EDS analysis. Two crystallographically unique uranyl cations are present in this structure; two oxo atoms are found along in the axial positions. The four sites in the equatorial plane of the first uranium center consist of oxygen atoms from the diphosphonate ligand, while one of the four sites is occupied by a water molecule in the second uranium center. The $PO_3$ moieties play two important roles in the structure: they span between the uranyl cations to help

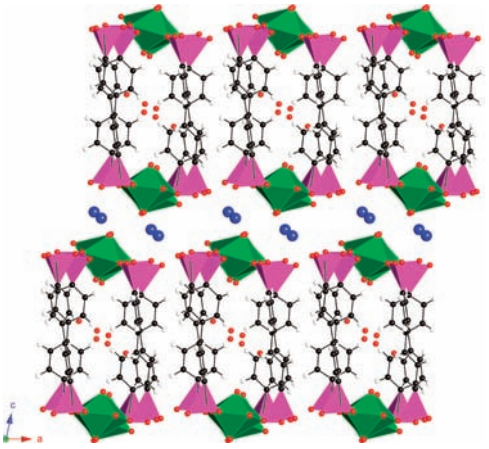

**Figure 3.** View down the *b* axis of $M_2\{(UO_2)_2F(PO_3HC_6H_4C_6H_4PO_3H)(PO_3HC_6H_4C_6H_4PO_3)\}\cdot 2H_2O$ ($M = Cs^+$ and $Rb^+$) showing the packing of the uranyl diphosphonate nanotubules. $UO_6F$ pentagonal bipyramids = green, cesium = blue, oxygen = red, phosphorus = magenta, carbon = black, hydrogen = white.

create the dimers and also bridge between the dimers to create one-dimensional chains that extend along the length of the nanotubules. This topology is similar to what we reported earlier and in uranyl molybdates[12] except that one of the phosphonates moieties is not involved in connecting the chains or the dimers. One such chain exists in the structure, and they are connected by the biphenyl rings to create the tubular channels that are filled by disordered water molecules. The nanotubules are anionic. Some of the charge is compensated by protonating terminal P−O groups as indicated by the formula, and the $Cs^+/Rb^+$ cations that are located between the nanotubules as shown in the packing diagram in Figures 3 and 4. The key feature that this nanotubular structure creates is different chemical environments within ($H_2O$ molecules) and outside ($Cs^+$ ions) of the tubes. The Cs(1) cations outside the tubes are bound by water molecules, fluoride, two oxo atoms from the uranyl cations, and five phosphonate oxygen atoms. While Cs(2) forms 11 long contacts with 3 oxo atoms from the uranyl cations and 8 phosphonate oxygen atoms. The U−O bond lengths for all the oxo atoms of the uranyl moieties that coordinated to Cs atoms slightly increased as shown in Tables 2 and 3. The Cs−O bond distances range from 3.032(4) to


dx.doi.org/10.1021/ic201945p | *Inorg. Chem.* 2011, 50, 12184–12191

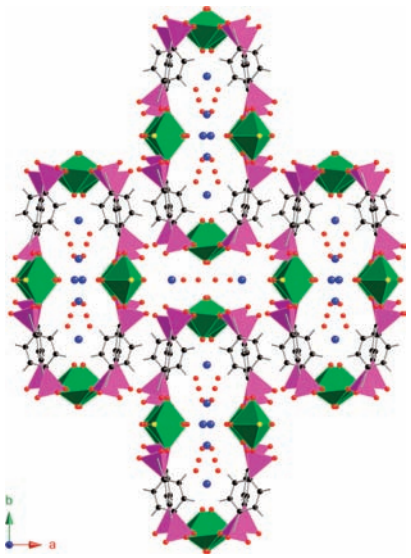

**Figure 4.** Illustration of the packing in $Cs_{3.62}H_{0.38}\{(UO_2)_4[C_6H_4(PO_2OH)_2]_3[C_6H_4(PO_3)_2]F_2\}\cdot nH_2O$ along the *c* axis. $UO_6F$ pentagonal bipyramids = green, cesium = blue, oxygen = red, phosphorus = magenta, fluorine = yellow, carbon = black, phenyl ring = gray.

**Table 2. Selected Bond Distances (Å) and Angles (deg) for $Rb_2\{(UO_2)_2F(PO_3HC_6H_4C_6H_4PO_3H)(PO_3HC_6H_4C_6H_4PO_3)\}\cdot 2H_2O$ (RbUbpbp-1)**

| | | | |
|---|---|---|---|
| | Distances (Å) | | |
| U(1)—O(1) | 1.770(3) | P(1)—O(8) | 1.509(3) |
| U(1)—O(2) | 1.799(3) | P(1)—O(7) | 1.572(3) |
| U(1)—O(11) | 2.299(3) | P(1)—C(1) | 1.778(5) |
| U(1)—O(17) | 2.317(3) | P(2)—O(11) | 1.514(3) |
| U(1)—F(1) | 2.334(3) | P(2)—O(9) | 1.523(4) |
| U(1)—O(8) | 2.374(3) | P(2)—O(10) | 1.552(4) |
| U(1)—O(13) | 2.393(3) | P(2)—C(10) | 1.787(5) |
| U(2)—O(3) | 1.774(4) | P(3)—O(13) | 1.514(3) |
| U(2)—O(4) | 1.786(3) | P(3)—O(14) | 1.515(3) |
| U(2)—F(1) | 2.267(3) | P(3)—O(12) | 1.578(3) |
| U(2)—O(6) | 2.323(3) | P(3)—C(13) | 1.793(5) |
| U(2)—O(15) | 2.333(3) | P(4)—O(17) | 1.500(3) |
| U(2)—O(14) | 2.387(3) | P(4)—O(15) | 1.517(3) |
| U(2)—O(5) | 2.495(3) | P(4)—O(16) | 1.570(3) |
| P(1)—O(6) | 1.508(3) | P(4)—C(22) | 1.795(5) |
| | Angles (deg) | | |
| O(1)—U(1)—O(2) | 178.07(15) | O(3)—U(2)—O(4) | 179.20(16) |

3.760(4) Å. The bond-valence sums for both **CsUbpbp-1** and **RbUbpbp-1** are 5.91 to 5.99 for U(1) and U(2), which are consistent with U(VI).[13] Selected bond distances and angles are given in Tables 2 and 3.

**Spectroscopic Characterization.** The absorbance spectra **CsUbpbp-1** and **RbUbpbp-1** were collected from single crystals using a microspectrophotometer. These spectra are provided in the Supporting Information, and show the characteristic equatorial U—O charge transfer bands and axial U═O charge transfer bands (vibronic coupling) near 330 and 425 nm, respectively. The charge-transfer based emission is vibronically coupled to both bending and stretching modes of the uranyl cation, and typically consists of a five-peak spectrum, although far more lines can be observed at low temperature.[14a] Denning and his group members have examined in detail these transitions for the solid samples containing the $[UO_2Cl_4]^{2-}$ anion owing to its crystallization in a

**Table 3. Selected Bond Distances (Å) and Angles (deg) for $Cs_2\{(UO_2)_2F(PO_3HC_6H_4C_6H_4PO_3H)(PO_3HC_6H_4C_6H_4PO_3)\}\cdot 2H_2O$ (CsUbpbp-1)**

| | | | |
|---|---|---|---|
| | Distances (Å) | | |
| U(1)—O(1) | 1.766(4) | P(1)—O(8) | 1.531(4) |
| U(1)—O(2) | 1.807(4) | P(1)—O(7) | 1.533(4) |
| U(1)—O(6) | 2.300(3) | P(1)—C(1) | 1.798(6) |
| U(1)—O(15) | 2.320(4) | P(2)—O(9) | 1.502(4) |
| U(1)—F(1) | 2.347(3) | P(2)—O(11) | 1.514(4) |
| U(1)—O(9) | 2.369(4) | P(2)—O(10) | 1.570(4) |
| U(1)—O(14) | 2.390(4) | P(2)—C(10) | 1.788(5) |
| U(2)—O(3) | 1.764(4) | P(3)—O(13) | 1.515(4) |
| U(2)—O(4) | 1.794(4) | P(3)—O(14) | 1.520(4) |
| U(2)—F(1) | 2.263(3) | P(3)—O(12) | 1.575(4) |
| U(2)—O(11) | 2.294(4) | P(3)—C(13) | 1.805(6) |
| U(2)—O(13) | 2.363(3) | P(4)—O(15) | 1.503(4) |
| U(2)—O(17) | 2.365(4) | P(4)—O(17) | 1.525(4) |
| U(2)—O(5) | 2.579(4) | P(4)—O(16) | 1.565(4) |
| P(1)—O(6) | 1.523(4) | P(4)—C(22) | 1.795(5) |
| | Angles (deg) | | |
| O(1)—U(1)—O(2) | 178.25(16) | O(3)—U(2)—O(4) | 178.18(17) |

cubic space group.[14b] However, not all uranyl compounds possess luminescence properties, and the mechanisms of the emission from uranyl compounds are most often difficult to explain. The fluorescence spectrum for **CsUbpbp-1** and **RbUbpbp-1** are alike and are shown in the Supporting Information. The luminescence spectra of **CsUbpbp-1** and **RbUbpbp-1** differ only in the peak resolution: this is likely due to the sizes and quality of the crystals examined. Five prominent peaks are clearly resolved that correspond to electronic and vibronic transitions $S_{11}-S_{00}$ and $S_{10}-S_{0v}$ ($v = 0-4$). The most intense peak is positioned at 543 nm for these two compounds. These compounds exhibit a slight red shift of 35 nm along with lesser intensity for the emission bands compared to $UO_2(NO_3)_2\cdot 6H_2O$.[9a,b,d–f] The slight difference from these two compounds and the benchmark compound may be attributed to the coordination environment around uranium center, $UO_6F$, and the effect of the ligand.

The low wavenumber region of the IR spectra (see Supporting Information), from 675 to 715 $cm^{-1}$ is dominated by the O—P—O bending, phenyl ring and P—C stretching vibrations. The asymmetric and symmetric stretching modes of the uranyl cation, $UO_2^{2+}$, range from about 810—910 $cm^{-1}$. The group of peaks around 1000—1181 $cm^{-1}$ is at expected values for P—O and P═O symmetric and asymmetric stretching modes of phosphonates. The bands between 1391—1490 $cm^{-1}$ are due to phenyl ring stretching vibrations. The peaks around 2700 $cm^{-1}$ are indicative of the C—H stretching in the phenyl ring.[15–17]

**Thermogravimetric Analysis.** The weight loss for $M_2\{(UO_2)_2F(PO_3HC_6H_4C_6H_4PO_3H)(PO_3HC_6H_4C_6H_4PO_3)\}\cdot 2H_2O$ ($M = Cs^+$ and $Rb^+$) occurred in two steps (see Supporting Information), the first of which (~3%) took place between approximately 130 to 200 °C, which corresponds to the loss of water molecules. The second step began at about 320 °C and was complete by 820 °C and can be attributed to the decomposition of the biphenylenebisphosphonate ligand.

**Ion-Exchange Studies with $M_2\{(UO_2)_2F(PO_3HC_6H_4C_6H_4PO_3H)(PO_3HC_6H_4C_6H_4PO_3)\}\cdot 2H_2O$ ($M = Cs^+$ and $Rb^+$).** The presence of cations between the nanotubules makes **CsUbpbp-1** and **RbUbpbp-1** suitable candidates for ion-exchange studies. **CsUbpbp-1** exhibits different behaviors toward selected


dx.doi.org/10.1021/ic201945p | *Inorg. Chem.* 2011, 50, 12184–12191

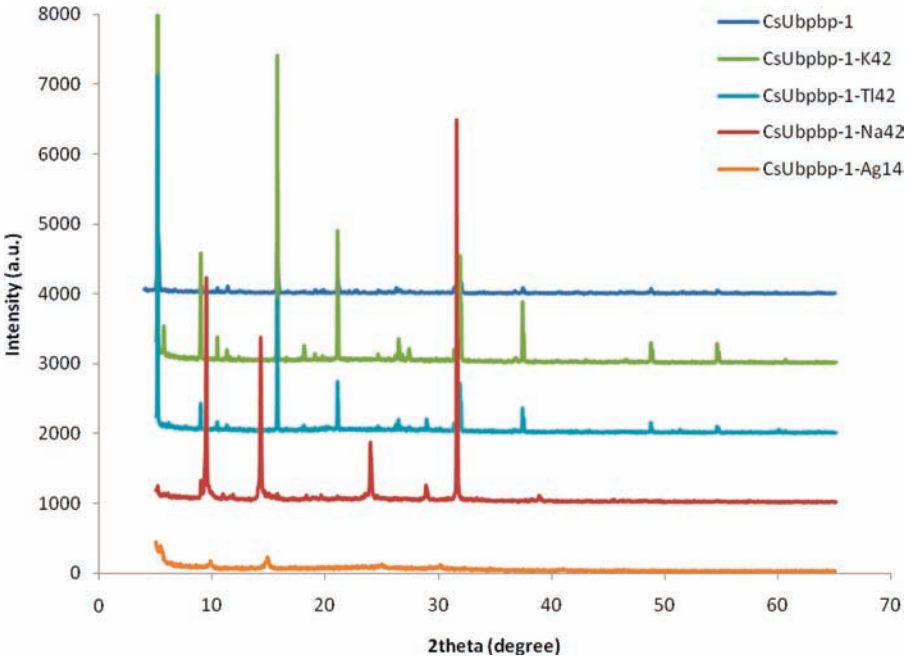


**Figure 5.** Powder XRD patterns in $M_2\{(UO_2)_2F(PO_3HC_6H_4C_6H_4PO_3H)(PO_3HC_6H_4C_6H_4PO_3)\}\cdot 2H_2O$ structure before and after ion-exchange experiment with $Na^+$, $K^+$, $Tl^+$ (42 days), and $Ag^+$ (14 days) cations.

monovalent and divalent cations ($Na^+$, $K^+$, $Tl^+$, $Ag^+$, and $Sr^{2+}$). The EDS studies reveal that $Ag^+$ ions were exchanged for the $Cs^+$ ions between the nanotubules in less than a week while investigations toward the other cations did not yield any ion-exchange. Because of poor crystallinity, we could not examine the crystals further using single crystal XRD, but the powder XRD result (Figure 5) shows that the basic framework has rearranged upon ion-exchange process with $Ag^+$ cations. The crystals began to fall apart (turned to a black precipitate or powder) after two weeks in the $Ag^+$ aqueous solution. The powder pattern of $Ag^+$ exchanged products is similar to what we observed in our study with $Na^+$ ions as shown in Figure 5. Results of the powder pattern from our investigation with $K^+$, $Tl^+$, and $Sr^{2+}$ show a pattern similar to that of the as-synthesized **CsUbpbp-1** compound. We also noticed some improvement in the quality of the crystal in the vials used for ion-exchange studies after about 6 weeks. These suggest that these materials likely dissolved and reprecipitated, providing us some clues to the possible mechanism of the exchange process.[18] The reason for this behavior might be due to the coordinating water molecule and unidentate $PO_3$ moiety around the uranium center that are labile as shown in Figure 2a.

**Ion-Exchange Studies with $Cs_{3.62}H_{0.38}\{(UO_2)_4[C_6H_4(PO_2OH)_2]_3[C_6H_4(PO_3)_2]F_2\}\cdot nH_2O$ (CsUbbp-1).** The disordered state and partial occupancy of the $Cs^+$ ions in **CsUbbp-1** imply ion mobility and good ion-exchange properties. While the different chemical environment around $Cs^+$ within and outside the tubes points toward differential ion-exchange rate. We have initially demonstrated the ion-exchange properties of ground **CsUbbp-1** with the $Ag^+$ ion.[2a] The results show that the $Cs^+$ ions within the nanotubules were completely exchanged within a week; we observed partial exchange because the cations between the tubes exchange at a slower rate. We ran further experiments with selected monovalent and divalent cations to probe whether the complete ion-exchanged product is prone to collapse since $Cs^+$ cation plays a vital role in controlling the assembly of uranyl diphosphonate into the nanotubular structure. First and foremost, we observed complete exchange of $Cs^+$ ions with monovalent cations after an extended period of time, 60 days. The small amount of divalent ions ($Sr^{2+}$) detected in the crystals by SEM/EDS analysis can be attributed to adsorption on the surface of the sample. Interestingly, the selectivity for monovalent ions is remarkable, as absolute selectivity is uncommon in hybrid inorganic–organic open framework ion-exchange materials which tend to relate more on sizes than charges.[19] The EDS analysis showed some trend in the amount of monovalent ions that were exchanged for the $Cs^+$ ions as follows, $Na^+ < K^+ \leq Ag^+ \leq Tl^+$. The reason why sodium was partially exchanged was because of the large hydration sphere of the alkali metal ions. The ion-exchange process with $Tl^+$ ions occurred in a shorter time (31 days) compared to other cations (60 days) because of the modification of the experimental conditions: the ion-exchange was investigated at 70 °C using a magnetic stirrer because of low solubility of thallium nitrate in water (see Figure 7). The structure changed slightly as shown by the powder XRD pattern as shown in Figure 6. It shows that **CsUbbp-1** contains certain voids that are suitably sized for $Cs^+$ ($r$ = 1.88 Å) and other cations appear to be too small or large (considering hydration of alkali metals), $Na^+$ ($r$ = 1.39), $K^+$ ($r$ = 1.64), $Ag^+$ ($r$ = 1.28), $Tl^+$ ($r$ = 1.70).[20] There seems to be an expansion/contraction phenomenon in which water molecules and smaller sized cations were absorbed into the framework of **CsUbbp-1**. The crystal quality was poor thus we were unable to collect suitable single crystal XRD data, but there was an evidence that the tubes remained intact. The structural changes observed here did not result in permanent collapse of the elliptical tubes in **CsUbbp-1** because reversible ion-exchange with $Cs^+$ led to isolation of as-synthesized material. The ion-exchange process with the exchange products of $Tl^+$ ions (5 days) and $Ag^+$ ions (3 weeks) resulted in **CsUbbp-1**, demonstrating the reversible ion-exchange property for regenerating these materials.


dx.doi.org/10.1021/ic201945p | Inorg. Chem. 2011, 50, 12184–12191

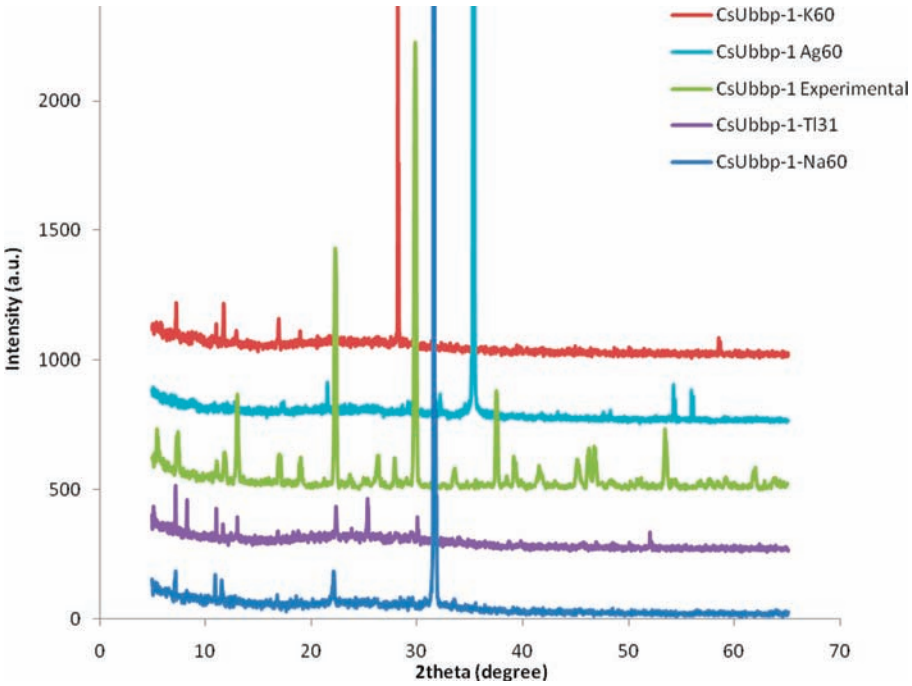


**Figure 6.** Powder XRD patterns in $Cs_{3.62}H_{0.38}\{(UO_2)_4[C_6H_4(PO_2OH)_2]_3[C_6H_4(PO_3)_2]F_2\}$ structure before and after ion-exchange experiment with $Na^+$, $K^+$, $Ag^+$ (60 days), and $Tl^+$ (31 days) cations.

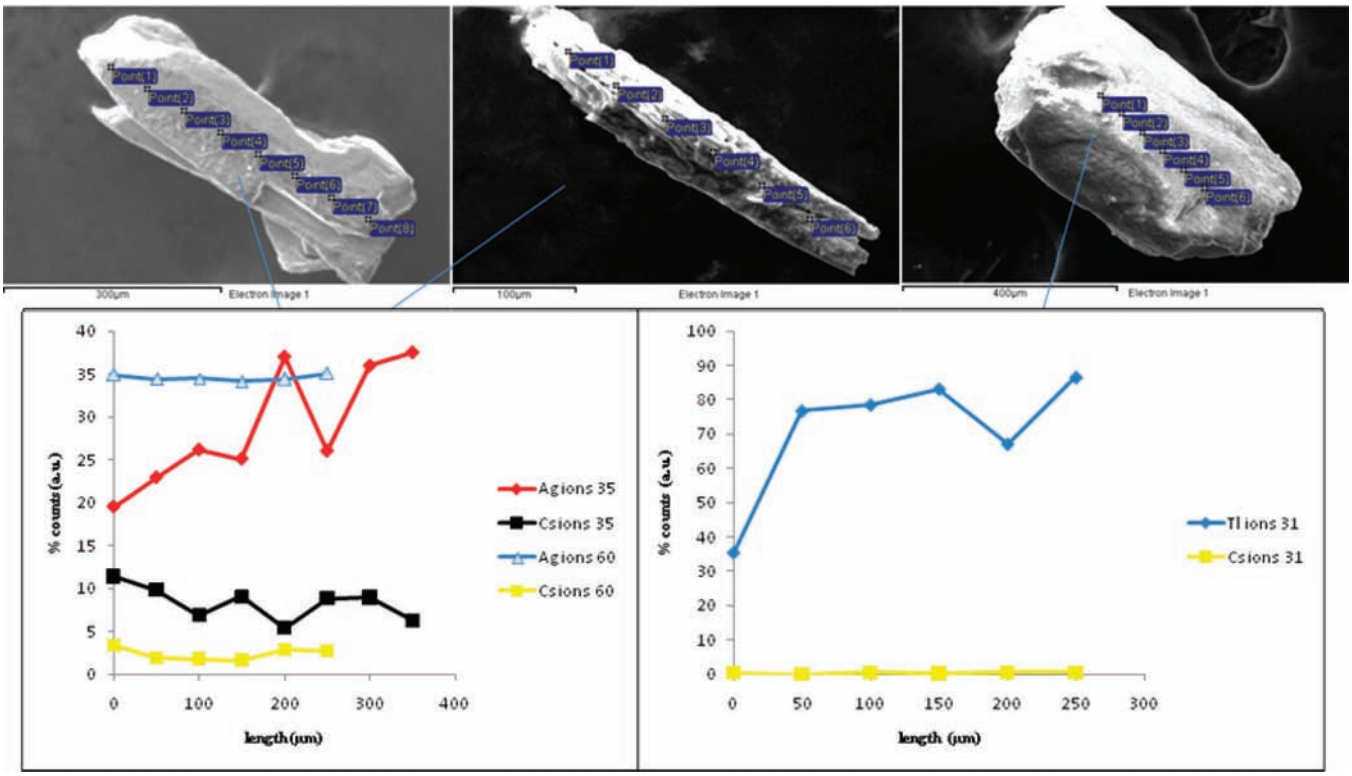


**Figure 7.** SEM image of the single crystal; the spots indicate areas where EDS patterns were collected (top). Plots of the fractional occupancies (% counts) of $Ag^+$, $Tl^+$, and $Cs^+$ ions against the distances on partial to complete exchange products. Data point connectors are for visual effect only.

**Implications of Single Crystal Studies coupled with SEM/EDS Results for the Ion Exchange Mechanism.** We monitored changes on the batch exchange samples from the first day and studied the partial and complete exchange products using SEM/EDS analysis and single crystal XRD. Because of the slow rate of substitution of the cations in the **CsUbbp-1** samples in aqueous solutions, we were able to collect the crystals in batches and examined the compositions of $Cs^+$ and $Ag^+/Tl^+$ cations. Significantly, the EDS analysis from partially exchanged samples as shown in the Supporting Information, reveal compositional variations as a function of distances. Thus, we found an evidence for chemical zonation, as


dx.doi.org/10.1021/ic201945p | *Inorg. Chem.* 2011, 50, 12184–12191

we might expect for exchange through diffusion mechanism.[18] These variations of the concentration of cations with distances in the ion-exchanged crystals decreased as we approach complete exchanged products (Figure 7).

## CONCLUSIONS

The foregoing results demonstrate the use of the complex and large oxoanions such as 1,4-phenyldiphosphonate and biphenylenebisphosphonate to construct uranyl nanotubules. These nanotubules are robust, and the single crystals withstand ion exchange without degradation of their crystallinity. They retain their integrity even with treatment at 70 °C, for a long period of 60 days and with reversible exchange of $Cs^+$ ions for another three weeks. All previous examples utilized smaller anions. The large linker between the uranyl cations yields elliptical nanotubules instead of ones with nearly circular cross sections.[2b−l] Moreover, **CsUbbp-1** represents the first highly stable functional uranyl nanotubule with exceptional ion-exchange properties. The single crystal studies with SEM/EDS provide an evidence for chemical zonation, as we might expect for exchange through diffusion mechanism. Such a remarkable combination of properties may open the way for testing uranyl nanotubules in a variety of other applications. We therefore conclude that uranyl nanotubules are not simply aesthetically pleasing architectures, but rather physicochemical property relationships that are derived from the differences of the chemical environments within and around the nanotubules.

## ASSOCIATED CONTENT

### Supporting Information

X-ray crystallographic files in CIF format for $M_2\{(UO_2)_2F(PO_3HC_6H_4C_6H_4PO_3H)(PO_3HC_6H_4C_6H_4PO_3)\}\cdot 2H_2O$ (M = $Cs^+$ and $Rb^+$) (**CsUbpbp-1** and **RbUbpbp-1**), and $Cs_{3.62}H_{0.38}\{(UO_2)_4[C_6H_4(PO_2OH)_2]_3[C_6H_4(PO_3)_2]F_2\}\cdot nH_2O$ (**CsUbbp-1**). Powder XRD patterns, spectroscopic data, and SEM/EDS data are also available. This material is available free of charge via the Internet at http://pubs.acs.org.

## AUTHOR INFORMATION

### Corresponding Author

*E-mail: talbrec1@nd.edu.

## ACKNOWLEDGMENTS

This work was supported by the Chemical Sciences, Geosciences and Biosciences Division, Office of Basic Energy Sciences, Office of Science, Heavy Elements Program, U.S. Department of Energy under Grant DE-SC0002215.

## REFERENCES

(1) (a) Burns, P. C.; Miller, M. L.; Ewing, R. C. *Can. Mineral.* **1996**, *34*, 845. (b) Burns, P. C. In *Uranium: Mineralogy, Geochemistry and the Environment*; Burns, P. C., Finch, R., Eds.; Mineralogical Society of America: Washington, DC, 1999; Chapter 1. (c) Burns, P. C. *Mater. Res. Soc. Symp. Proc.* **2004**, *802*, 89. (d) Burns, P. C. *Can. Mineral.* **2005**, *43*, 1839.

(2) (a) Adelani, P. O.; Albrecht-Schmitt, T. E. *Angew. Chem., Int. Ed.* **2010**, *49*, 8909. (b) Mihalcea, I.; Henry, N.; Loiseau, T. *Cryst. Growth Des.* **2011**, *11*, 1940. (c) Albrecht-Schmitt, T. E. *Angew. Chem., Int. Ed.* **2005**, *44*, 4836. (d) Thuery, P. *Inorg. Chem. Commun.* **2008**, *11*, 616. (e) Krivovichev, S. V.; Kahlenberg, V.; Kaindl, R.; Mersdorf, E.; Tananaev, I. G.; Myasoedov, B., F. *Angew. Chem., Int. Ed.* **2005**, *44*, 1134. (f) Krivovichev, S. V.; Kahlenberg, V.; Tananaev, I. G.; Kaindl, R.; Mersdorf, E.; Myasoedov, B. F. *J. Am. Chem. Soc.* **2005**, *127*, 1072. (g) Poojary, D. M.; Grohol, D.; Clearfield, A. *Angew. Chem., Int. Ed.* **1995**, *34*, 1508. (h) Poojary, D. M.; Cabeza, A.; Aranda, M. A. G.; Bruque, S.; Clearfield, A. *Inorg. Chem.* **1996**, *35*, 1468. (i) Grohol, D.; Clearfield, A. *J. Am. Chem. Soc.* **1997**, *119*, 9301. (j) Aranda, M. A. G.; Cabeza, A.; Bruque, S.; Poojary, D. M.; Clearfield, A. *Inorg. Chem.* **1998**, *37*, 1827. (k) Grohol, D.; Subramanian, M. A.; Poojary, D. M.; Clearfield, A. *Inorg. Chem.* **1996**, *35*, 5264. (l) Alekseev, E. V.; Krivovichev, S. V.; Depmeier, W. *Angew. Chem., Int. Ed.* **2008**, *47*, 549.

(3) (a) Kubatko, K. A. H.; Helean, K. B.; Navrotsky, A.; Burns, P. C. *Science* **2003**, *302*, 1191. (b) Burns, P. C.; Kubatko, K. A.; Sigmon, G.; Fryer, B. J.; Gagnon, J. E.; Antonio, M. R.; Soderholm, L. *Angew. Chem., Int. Ed.* **2005**, *44*, 2135. (c) Ling, J.; Qiu, J.; Sigmon, G. E.; Ward, M.; Szymanowski, J. E. S.; Burns, P. C. *J. Am. Chem. Soc.* **2010**, *132*, 13395. (d) Unruh, D. K.; Burtner, A.; Pressprich, L.; Sigmon, G. E.; Burns, P. C. *Dalton Trans.* **2010**, *39*, 5807. (e) Sigmon, G. E.; Ling, J.; Unruh, D. K.; Moore-Shay, L.; Ward, M.; Weaver, B.; Burns, P. C. *J. Am. Chem. Soc.* **2009**, *131*, 16648. (f) Sigmon, G. E.; Weaver, B.; Kubatko, K.; Burns, P. C. *Inorg. Chem.* **2009**, *48*, 10907. (g) Unruh, D. K.; Burtner, A.; Burns, P. C. *Inorg. Chem.* **2009**, *48*, 2346. (h) Soderholm, L.; Almond, P. M.; Skanthakumar, S.; Wilson, R. E.; Burns, P. C. *Angew. Chem., Int. Ed.* **2008**, *47*, 298. (i) Ling, J.; Qiu, J.; Szymanowski, J. E. S.; Burns, P. C. *Chem.—Eur. J.* **2011**, *17*, 2571. (j) Ling, J.; Wallace, C. M.; Szymanowski, J. E. S.; Burns, P. C. *Angew. Chem., Int. Ed.* **2010**, *49*, 7271.

(4) (a) Nash, K. L. *J. Alloys Cmpd.* **1994**, *213-214*, 300. (b) Nash, K. L. *J. Alloys Cmpd.* **1997**, *249*, 33. (c) Jensen, M. P.; Beitz, J. V.; Rogers, R. D.; Nash, K. L. *J. Chem. Soc., Dalton Trans.* **2000**, *18*, 3058.

(5) (a) Dieckmann, G. H.; Ellis, A. B. *Solid State Ionics* **1989**, *32/33*, 50. (b) Vochten, R. *Am. Mineral.* **1990**, *75*, 221. (c) Benavente, J.; Ramos Barrado, J. R.; Cabeza, A.; Bruque, S.; Martinez, M. *Colloids Surf., A* **1995**, *97*, 13. (d) Shvareva, T. Y.; Almond, P. M.; Albrecht-Schmitt, T. E. *J. Solid State Chem.* **2005**, *178*, 499. (e) Shvareva, T. Y.; Sullens, T. A.; Shehee, T. C.; Albrecht-Schmitt, T. E. *Inorg. Chem.* **2005**, *44*, 300. (f) Shvareva, T. Y.; Skanthkumar, S.; Soderholm, L.; Clearfield, A.; Albrecht-Schmitt, T. E. *Chem. Mater.* **2007**, *19*, 132. (g) Ok, K. M.; Baek, J.; Halasyamani, P. S. *Inorg. Chem.* **2006**, *45*, 10207.

(6) (a) Grohol, D.; Blinn, E. L. *Inorg. Chem.* **1997**, *36*, 3422. (b) Johnson, C. H.; Shilton, M. G.; Howe, A. T. *J. Solid State Chem.* **1981**, *37*, 37. (c) Moreno-Real, L.; Pozas-Tormo, R.; Martinez-Lara, M.; Bruque-Gamez, S. *Mater. Res. Bull.* **1987**, *22*, 29. (d) Pozas-Tormo, R.; Moreno-Real, L.; Martinez-Lara, M.; Rodriguez-Castellon, E. *Can. J. Chem.* **1986**, *64*, 35. (e) Obbade, S.; Dion, C.; Saadi, M.; Abraham, F. *J. Solid State Chem.* **2004**, *177*, 1567. (f) Obbade, S.; Duvieubourg, L.; Dion, C.; Abraham, F. *J. Solid State Chem.* **2007**, *180*, 866.

(7) (a) Almond, P. M.; Talley, C. E.; Bean, A. C.; Peper, S. M.; Albrecht-Schmitt, T. E. *J. Solid State Chem.* **2000**, *154*, 635. (b) Frisch, M.; Cahill, C. L. *Dalton Trans.* **2006**, *39*, 4679. (c) Cahill, C. L.; de Lill, D. T.; Frisch, M. *CrystEngComm* **2007**, *9*, 15.

(8) (a) Sykora, R. E.; Albrecht-Schmitt, T. E. *Inorg. Chem.* **2003**, *47*, 2179. (b) Cao, G.; Hong, H.-G.; Mallouk, T. E. *Acc. Chem. Res.* **1992**, *25*, 420. (c) Clearfield, A. *Curr. Opin. Solid State Mater. Sci.* **2003**, *6*, 495. (d) Mao, J.-G. *Coord. Chem. Rev.* **2007**, *251*, 1493.

(9) (a) Adelani, P. O.; Albrecht-Schmitt, T. E. *Inorg. Chem.* **2010**, *49*, 5701. (b) Adelani, P. O.; Albrecht-Schmitt, T. E. *Inorg. Chem.* **2009**, *48*, 2732. (c) Adelani, P. O.; Oliver, A. G.; Albrecht-Schmitt, T. E. *Cryst. Growth Des.* **2011**, *11*, 1966. (d) Adelani, P. O.; Oliver, A. G.; Albrecht-Schmitt, T. E. *Cryst. Growth Des.* **2011**, *11*, 3072. (e) Adelani, P. O.; Albrecht-Schmitt, T. E. *Cryst. Growth Des.* **2011**, *11*, 4227. (f) Adelani, P. O.; Albrecht-Schmitt, T. E. *Cryst. Growth Des.* **2011**, *11*, 4676. (g) Adelani, P. O.; Albrecht-Schmitt, T. E. *J. Solid State Chem.* **2011**, *184*, 2368.

(10) (a) Clearfield, A. *Prog. Inorg. Chem.* **1998**, *47*, 371. (b) Grohol, D.; Clearfield, A. *J. Am. Chem. Soc.* **1997**, *119*, 4662. (c) Dines, M. B.; Griffith, P. C. *Polyhedron* **1983**, *2*, 607. (d) Karthikeyan, S.; Paine, R. T.; Ryan, R. R. *Inorg. Chim. Acta* **1988**, *144*, 135. (e) Cromer, D. T.; Ryan, R. R.; Karthikeyan, S.; Paine, R. T. *Inorg. Chim. Acta* **1990**, *172*, 165. (f) Henderson, W.; Leach, M. T.; Nicholson, B. K.; Wilkins, A. L.; t. l. Hoye, P. A. T. *Polyhedron* **1998**, *17*, 3747. (g) Doran, M. B.; Norquist, A. J.; O'Hare, D. *Chem. Mater.* **2003**, *15*, 1449.

(11) (a) Sheldrick, G. M. *SADABS*, Program for absorption correction using SMART CCD based on the method of Blessing: Blessing, R. H. *Acta Crystallogr.* **1995**, *A51*, 33. (b) Sheldrick, G. M. *SHELXTL PC*, Version 6.12, An Integrated System for Solving, Refining, and Displaying Crystal Structures from Diffraction Data; Siemens Analytical X-Ray Instruments, Inc.: Madison, WI, 2001.
(12) (a) Krivovichev, S. V.; Burns, P. C. *J. Solid State Chem.* **2002**, *168*, 245. (b) Krivovichev, S. V.; Burns, P. C. *Can. Mineral.* **2001**, *39*, 197.
(13) (a) Brese, N. E.; O'Keeffe, M. *Acta Crystallogr.* **1991**, *B47*, 192. (b) Burns, P. C.; Ewing, R. C.; Hawthorne, F. C. *Can. Mineral.* **1997**, *35*, 1551.
(14) (a) Liu, G.; Beitz, J. V. In *The Chemistry of the Actinide and Transactinide Elements*; Morss, L. R., Edelstein, N. M., Fuger, J., Eds.; Springer: Heidelberg, Germany, 2006; p 2088. (b) Denning, R. G.; Norris, J. O. W.; Short, I. G.; Snellgrove, T. R.; Woodwark, D. R. *Lanthanide and Actinide Chemistry and Spectroscopy*; ACS Symposium Series 131; American Chemical Society: Washington, DC, 1980.
(15) Grohol, D.; Subramanian, M. A.; Poojary, D. M.; Clearfield, A. *Inorg. Chem.* **1996**, *35*, 5264.
(16) Knope, K. E.; Cahill, C. L. *Inorg. Chem.* **2008**, *47*, 7660.
(17) Knope, K. E.; Cahill, C. L. *Inorg. Chem.* **2009**, *48*, 6845.
(18) (a) Fewox, C. S.; Kirumakki, S. R.; Clearfield, A. *Chem. Mater.* **2007**, *19*, 384. (b) Lopano, C. L.; Heaney, P. J.; Post, J. E. *Am. Mineral.* **2009**, *94*, 816. (c) Fewox, C. S.; Clearfield, A.; Celestian, A. J. *Inorg. Chem.* **2011**, *50*, 3596.
(19) Plabst, M.; McCusker, L. B.; Bein. *J. Am. Chem. Soc.* **2009**, *131*, 18112.
(20) Shannon, R. *Acta Crystallogr., Sect. A* **1976**, *32*, 751.